PREPRINT UCRL- 82137 REV.1

Lawrence Livermore Laboratory

ATOMLLL: - ATOMS WITH SHADING AND HIGHLIGHTS

N.L. Max

May 11, 1979

This paper was prepared for Journal of Association for Computing Machinery
CHICAGO, IL AUGUST 6-10,1979

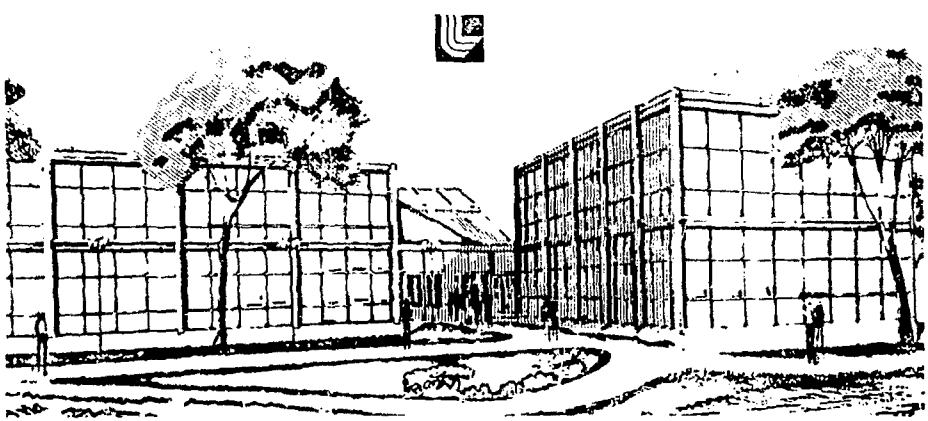

ATOMLLL: - ATOMS with Shading and Highlights

Nelson L. Max

Lawrence Livermore Laboratory

Abstract

The ATOMS program, written at Bell Telephone Laboratory, is capable of determining the the visible portions of a scene consisting of interpenetrating spheres and cylinders, put together to represent "space-filling" or "ball-and-stick" molecular models. The Lawrence Livermore Laboratory version contains enhancements to add shading and highlights, and to render the spheres on film as ellipses, so they will appear round when projected in various wide-screen formats.

The visible parts of each sphere or cylinder are shaded by a minicomputer controlling the film recorder, thus releasing the main computer from transferring the millions of intensity values for each frame. The minicomputer is microprogrammed with an efficient algorithm for the intensities, which uses the color look-up tables in the film recorder to store the reflectance as a function of angle of incidence.

Key Words and Phrases

Computer animation, shading, highlights, raster graphics, space-filling molecular models

CR Catagories

8.2, 3.13

1. Introduction

The ATOMS program (5), by Kenneth Knowlton and Lorinda Cherry at Bell Telephone Laboratory, computes the visible regions of a scene consisting of potentially intersecting spheres or cylinders, called parts. The ATOMLLL version runs on the CDC 7600 at Lawrence Livermore Laboratory. Its input is a list of atomic coordinates, radii, and colors, and a connection table for the bonds, if any. Its output is a binary tape containing shading information for each part, followed by a list of "trapezoids" into which the part has been divided, as described in Sec. 2.

This tape is read by a Varian V-75 minicomputer, which controls a Dicomed D-48 color film recorder. The Varian divides each trapezoid into vertical raster segments, and uses an efficient algorithm described in Sec. 3 to find the shading values along each segment, which are then plotted by the Dicomed. The most complex figures shown here took about 2 seconds on the 7600 to compute and output the visible surface parts, and 2 minutes on the Varian - Dicomed system to compute and plot the shading at 1536 x 2048 pixel resolution. Users can view the outlines of each part on a black and white TV monitor in their offices, while composing a sequence on the CDC 7600, before committing it to film (See Fig. 17).

Similar pictures have been produced by Thomas Porter (8), and John Staudhammer (9), using color video output. Porter's system can create pictures on a stand-alone PDP-11 minicomputer. Because it uses a depth buffer algorithm, several Z computations and comparisons may be required for each pixel. Staudhammer's system uses special purpose hardware to generate shading and highlights on the fly at video rates, from a previously prepared list of visible segments. His shading algorithm is based on a table, and is similar to the method reported here, although the actual table is quite different.

Both these systems currently output at the resolution of the standard color TV monitor. The ATOMLLL system can plot on wide format film at up to 4096 - 4096 resolution, giving much higher quality at the cost of extra plotting time, and can plot bonds as well as atoms. It is also capable of rendering the spheres on film as ellipses, as described in Sec. 4, to compensate for the distortion introduced by various wide screen projection lenses.

"Work performed under the auspices of the U.S. Department of Energy by the Lawrence Livermore Laboratory under contract number W-7405-ENG-48."

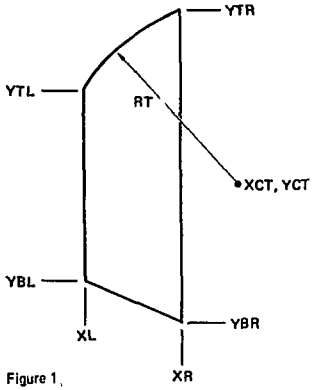

Figure 1

2. The Hidden Surface Algorithm

As described in (5), the ATOMLLL program keeps track of the visible portions of each part in terms of a list of "trapezoids". Each such trapezoid, as shown in Fig. 1, has two straight vertical sides. The other two sides may be straight lines or arcs of circles. The circular arcs can be convex down, as is the top arc in Fig. 1, or convex up. In addition, each arc must be monotone, with y either non-increasing or non-decreasing. Thus, a sphere is initially represented as two trapezoids, each having one degenerate vertical side, as shown in Fig. 2a.

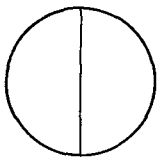

Figure 2a

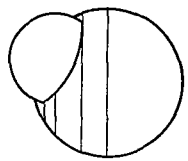

Figure 2b

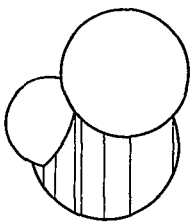

Figure 2c

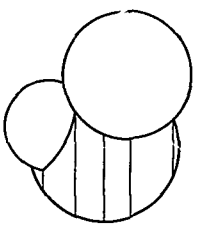

Figure 2d

If this sphere is intersected, or "truncated," by a second sphere, as in Fig. 2b, the intersection curve is approximated by a circular arc, and the trapezoids of the first sphere are chopped or subdivided into their visible pieces. They are further subdivided in Fig. 2c by a third atom in front of the other two. In general, the trapezoids in the currently visible list for a part can be compared one by one to the trapezoids defined for a potentially occluding part, and reduced or subdivided appropriately. A new modification may remove the reason for an earlier subdivision, as seen in Fig. 2c, where some of the vertical lines are no longer required. Thus, after any occlusion changes the list, it is compacted to amalgamate adjacent trapezoids if possible, as in Fig. 2d. Further details on the hidden surface algorithm can be found in (5) and (6).

3. Shading and Highlights

The shading algorithm is closely tied to several hardware features of the Dicomed D-48 film recorder. It contains a computer controlled color filter wheel, with six colors, and a seventh clear position. There are also eight loadable look-up tables, one to be used for each of the seven filter positions, and an eighth for black and white exposures. These tables translate an eight bit input intensity into another intensity for output onto the film, and were designed to compensate for film characteristics. In raster mode, the Dicomed gets a stream of bytes by direct memory access of an output buffer on the Varian, and plots the compensated values across a scan line. Meanwhile, the Varian may be filling a second buffer of intensities.

The atoms are shaded as if the light came from a point infinitely far behind the viewer. Thus the reflected intensity is a monotone decreasing function f(e), of the incidence angle e, shown in Fig. 3. For diffuse lighting, an appropriate intensity function might be

$$f(e) = A + D \cos e \qquad \ldots 1)$$

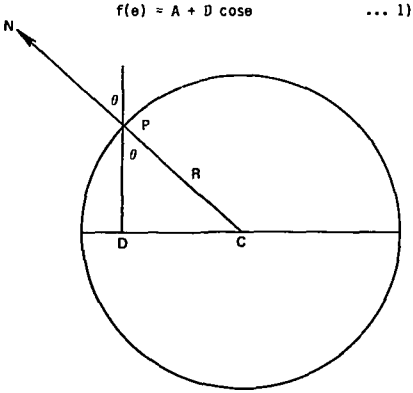

Figure 3

The color of the diffusely reflected light is the color of the surface.

For highlights, representing specular reflection concentrated at small incidence angles, an appropriate function might be

$$g(\theta) = C(\cos\theta)^n \qquad \ldots 2)$$

for some large n. The color of the highlight is white. The functions f(θ) and g(θ) are entered into the color and black-white look-up tables, respectively, so any reflection law may be used. More sophisticated functions are given in Blinn (1).

The functions f and g are actually tabulated in terms of $\cos^2\theta$. We now demonstrate how $\cos^2\theta$ can be computed very efficiently using finite differences.

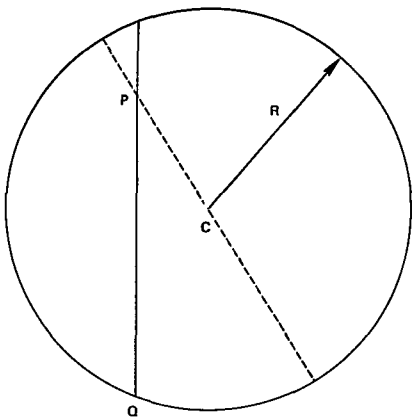

Figure 4

Figure 4 shows the projection of a sphere onto the picture plane. The point P=(X,Y,Z) is on the surface, C=(XC, YC, ZC) is the center, and R is the radius. Figure 3 shows a section of this sphere, in a plane perpendicular to the dotted line.

From triangle PDC in Fig. 3, we find

$$\cos^2\theta = \frac{\overline{PD}^2}{\overline{PC}^2} = \frac{(Z-ZC)^2}{R^2} \qquad \ldots 3)$$

Solving the equation of the sphere,

$$(X-XC)^2 + (Y-YC)^2 + (Z-ZC)^2 = R^2 \qquad \ldots 4)$$

for $(Z-ZC)^2$, and substituting in Eq. 3 we get

$$\cos^2\theta = \frac{R^2 - (X - XC)^2 - (Y - YC)^2}{R^2} \qquad \ldots 5)$$

Since the trapezoids have vertical sides, they are colored in vertical raster scan segments. Along a vertical segment such as the one shown in Fig. 4, the quantities R, X, XC, and YC are constant, so Eq. 5 represents a quadratic polynomial in Y. This polynomial is evaluated at successive points along the scan segment, using finite differences. The second difference for any quadratic polynomial is a constant, equal to its second derivative. Therefore, the exact value can be accumulated using two additions per cycle of the difference loop.

If N is the number of raster points to be plotted, the second difference is added effectively (N-1)(N-2)/2 times, so double precision integers are required on a 16 bit machine. Since the assembly language of the Varian does not permit more than one double precision operand to be retained in registers, the coding for the difference loop would be quite inefficient in memory access.

Fortunately, a writeable control store was available, so the whole loop was replaced by a new machine instruction written in microcode. Eight registers are loaded with N, the double precision values for $\cos^2\theta$ and its first and second differences at the bottom point Q of the scan segment, and the starting address of the output buffer. The microcode then does the two double precision adds, loads the high order byte of the accumulated value for $\cos^2\theta$ into the proper byte of the output buffer, tests for completion, and loops, all in eight 195 ns microinstruction cycles. For atoms which fill up a substantial area of the screen, it can generate the intensity values faster than the Dicomed can plot them. For smaller atoms, the square roots required for computing the upper and lower boundary arcs for the trapezoids become the bottleneck. They could be removed by using Bresenham's algorithm (2), as suggested in (8).

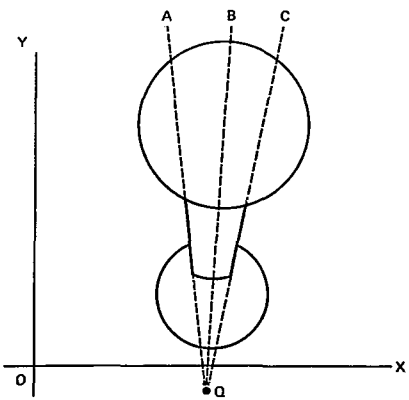

Figure 5

Ideally, the shading for a cylinder can also be determined from a quadratic polynomial along a vertical scan segment. However, after the perspective transformation, cylinders become cones, and the shading is no longer so simple, especially when the directions of the projected edges lie in different quadrants, as in Fig. 5.

Let Q be the "vanishing point" for these edges, so that QA and QC, the extentions of the projected edges, and QB, the projected center line, all meet at Q. Assume QA has negative slope, while QB and QC have positive slopes. Then the part of the bond lying in AQB will be shaded using quadratic polynomials on horizontal segments, and the part in BQC will be shaded using different polynomials on vertical segments. These polynomials are adjusted to have their maximum value (which depends on the angle between the bond axis and the plane of view) along the line QB, and to be zero along QA and QC. Thus they agree smoothly along QB, and give a close approximation to the true shading.

The usual method of color rendition represents the combined diffused and specular reflection as the sum of red, green, and blue components, painted in three separate passes through three colored filters. The present algorithm renders the diffuse reflection through one of the seven colored filters, using the look up table for $f(\cos^2\theta)$ and then adds the highlights through the clear filter, getting $g(\cos^2\theta)$ from the black and white table. In this way, only two passes are required, each with exactly the same data.

In summary, the combination of the finite difference technique for $\cos^2\theta$, with the look-up tables for the shading functions, results in a very efficient shading algorithm.

4. Wide Screen and Dome Projections

In early 1978, Lawrence Livermore Laboratory was approached by a group which proposed to produce computer animation in the IMAX(3), and OMNIMAX(4) wide screen movie formats. The film used is 70 mm wide, projected in a horizontal orientation, so that the larger dimension of the picture runs along 15 perforations of the film. Figure 6 shows a frame in full scale. It has more than 10 times the area of a 35 mm movie frame, permitting excellent resolution even when projected on a very wide screen. The IMAX format uses a 90° field-of-vi wide angle lens to project onto a huge slightly curved screen, while the OMNIMAX uses a 180° fi of view fisheye lens to project onto a hemisphe cal dome.

Both these systems introduce their own dist tions, which must be compensated for when plott on the film. In the IMAX format (see Fig. 15), image on the screen is a direct magnification c the image on the film. Nevertheless, because c forshortening, a sphere viewed from the center the theatre must be represented as an ellipse, whose long axis points toward the center of the screen. Near the corners of the screen, the el gation factor (ratio of long axis to short axis may be as great as 1.6. In the case of the OMN lens, which must distort a flat picture to cove the dome, the projection was chosen to concentr the high resolution near the center of the imag

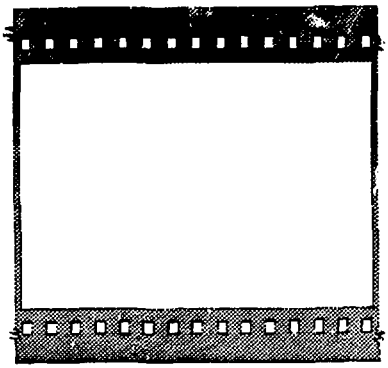

Figure 6 An IMAX movie frame.

and spread out a relatively small film area to cover the peripheral edges of the image, where human perception is not as precise. As a result, a sphere near the edge of the dome must be represented on film as an ellipse whose short axis points towards the center of the image, and whose elongation factor may be as large as 4.8 (see Fig. 16.)

We may put both these projections in the same conceptual framework by imagining a "dome of view", a unit hemisphere, with center at the projector and observer (assumed to coincide) which intercepts the rays headed for the screen. The characteristics of the projection lens determine the mapping between points P on the film, and their corresponding images Q on the dome of view.

Suppose P is represented, as in Fig. 7a, by the polar coordinates (r,θ), while Q is represented as in Fig. 7b, by the spherical coordinates (θ,ϕ). Then θ will equal θ, and the lens characteristics are represented by the function $\phi = \Phi(r)$. For the IMAX lense, $\Phi(r) = \arctan(r/r_0)$. For the OMNIMAX lens, $\Phi(r)$ is as plotted in Fig. 8, and was approximated by a polynomial in the computer.

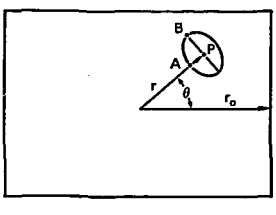

Figure 7a

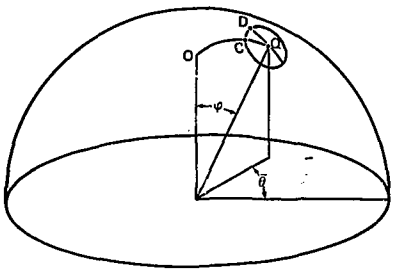

Figure 7b

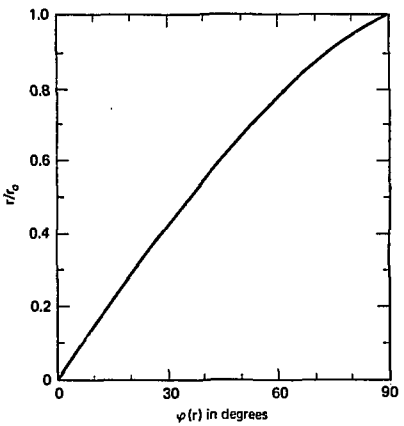

Figure 8

Now a small sphere in space will project onto a small round disk on the dome of view, with equal angular extents (CQ and QD) in the lattitude and longitude directions. Expressing these lengths in terms of the infinitesimals d and dθ, we get the equation

$$d\phi = \sin\phi\, d\theta \qquad \ldots 10)$$

To first order, the inverse image of this disk will be an ellipse in the film plane, with a semi-axis PB in the tangential direction, of length rdθ, and one in the radial direction, PA, of length dr. Their ratio, PB/PA=rdθ/dr is the elongation e(r). Solving Eq. 10 for dθ and subsituting, we find the elongation

$$e(r) = \frac{r d\theta}{dr} = \frac{r\, d\phi}{\sin\phi\, dr} = \frac{r}{\sin\phi}\,\phi'(r) \qquad \ldots 11)$$

If the function $\phi(r) = \cos^{-1}[(1-r^2)/(1+r^2)]$ is substituted into Eq. 11, the elongation turns out to be identically 1, and circles on the sphere map to circles (or straight lines) in the plane. This particular function is called stereographic projection, and is often used to map regions around the earth's poles, since it preserves the shape of land masses. In the case of the OMNIMAX projection, e(r) will be greater than one, since the ellipse is squashed in the radial direction by the inverse of the lens projection. For the IMAX lens, e(r) will be less than 1.

A sphere of finite size should usually have an egg shaped film image, since the general projection is non linear. However, the first order elliptical region, with orientation and elongation computed as in the infinitesimal case, is adequate. Inside such a region, the shading function $\cos^2\theta$ can be represented as a quadratic polynomial in X and Y, which vanishes at the boundary ellipse. Thus the shading can again be computed by finite differences along vertical scan segments. Note that θ here measures the direction of the normal vector to the atom before the distortion, so the shading will be correct after projection, and is not the correct shading for an ellipsoid.

The shading of the ellipses is simple enough, but the hidden surface algorithm is another question. Four person-years went into the algorithm of (5), which depends in two essential ways on circular arc boundaries.

The first is in a quick test to see whether two parts can interact in the picture plane. For example, two atoms do not interact if the sum of their projected radii does not exceed the distance between their projected centers. The structure of these quick tests was retained, by conducting them in sterographic coordinates, where spheres do project to circles.

Even these quick tests must be done N(N-1)/2 times for N parts, which would make the algorithm of order N^2. For large structures, the parts are therefore first sorted into lists corresponding to an array of film plane windows, so that parts which could possibly interact with a given part can be found in an appropriate subset of the lists.

The second dependence on circular arcs is in the algorithm which compares two trapezoids, and modifies one if it is occluded by the other. Here, elliptic boundaries could add substantial complication. For example two ellipses can intersect in as many as four points, while two circles can intersect in at most two.

Since the ellipse only approximates the egg shaped sphere projection, it was decided to approximate the ellipse boundary in turn by four circular arcs. The quadratic polynomial for the shading becomes negative for points outside the boundary ellipse. In order to avoid wraparound in the color look-up tables, the approximating arcs must thus remain inside or tangent to the ellipse, as shown in Fig. 9. The basic problem is to find the best approximation to the standard ellipse

$$\frac{X^2}{A^2} + Y^2 = 1 \qquad \ldots 12)$$

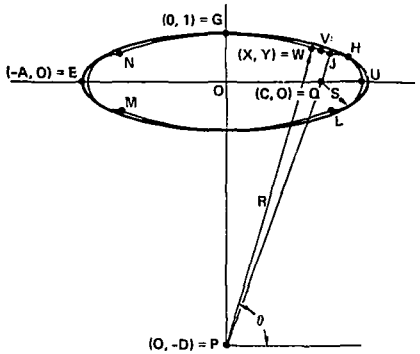

Figure 9. (Circular arcs distorted for clarity)

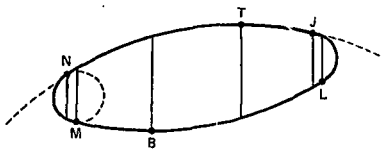

Figure 10

of elongation A>1. The approximation can then be rotated, translated, or magnified as required. A solution for the best approximation, which may be of use in other computer graphics applications requiring ellipses, is given in the Appendix.

Once the approximation is found it can be divided up into trapezoids, as shown in Fig. 10. Since the top and bottom points, T and B, need no longer have the same X coordinate, and we have introduced four new points of division, the initial subdivision will in general have seven trapezoids instead of two. After the trapezoids for a part are created, they may be modified as before by the trapezoids from a potentially occluding part.

Further complications are caused by the "truncation" arcs (see Fig. 2b), which are projections of the circles where two parts, say two spheres, intersect each other in space. The linear part of the perspective projection from space to the dome of view will turn such a circle into an ellipse. The linear part of the inverse projection from the dome through the lens onto the film, which we have just discussed, will then turn this ellipse into another ellipse. The equation for this "truncation" ellipse can be found by composing the linear parts of these two transformations. It can then be approximated by four circular arcs as before. In general, three of these arcs will be required to "truncate" an atom, and as many as 15 trapezoids may be generated. This process, which applies for the non-distorted projections as well, removes the corners seen in Fig. 2b.

5. The Film "DNA With Ethidium"

The public presentation includes a five minute computer animated film (7), produced at Lawrence Livermore Laboratory, illustrating the interaction of DNA with the drug ethidium bromide.

Ethidium is used as a fluorescent stain for DNA in cytological research. It is known to cause "frame" mutations in bacteria by being mistaken in its intercalated position (Fig. 12) for a base during DNA replication.

The film opens with six base pairs of DNA, rotating about the double helix axis. The computer simulates the "CPK space-filling molecular models," interlocking plastic spheres invented by Pauling and Corey to study chemical structure, and now in widespread use. Carbon atoms are dark blue rather than black, to stand out against the black background, but the other colors are standard: red for oxygen, white for hydrogen, blue for nitrogen and yellow for phosphous.

The rotation stops, and the DNA changes its conformation. The center two base pairs open up to twice their normal separation, and the other bases adjust by partially untwisting the helix (Fig. 11). The ethidium ion then moves into the gap that has been created i.e., "intercalates" (Fig. 12). The coordinates of the atoms during the interaction were calculated at Case Western Reserve University by Nelson Max and Deepak Malhotra. The CAMSEQ program, developed by Anton Hopfinger and his students, calculated the total interaction energies (including the effects of the surrounding water) for a large number of different positions, created to satisfy certain initial constraints, and the ones of minimum energy were chosen.

Work is continuing at Case-Western Reserve to refine these coordinates, and to calculate the interactions of DNA with other small molecules. The goal of this research is to learn to predict the mutagenicity and carcinogenicity of an arbitrary chemical compound, in order to select those compounds which are high priorities for expensive biological testing. Interactive computer graphics with space-filling models to show Van der Waals contacts could be a useful tool in this effort.

The next scene shows a dissolve between two different representations of the center two base pairs: the space-filling, and the ball-and-stick. When seen rotating, an intermediate stage in this dissolve gives the impression of a transparent outer electron shell, revealing the inner bond structure (Fig. 13).

The final scene shows a ball-and-stick representation of another local energy minimum for the DNA-ethidium interaction (Fig. 14), this time with the ethidium outside the "narrow grove."

Figure 15 shows in IMAX projection several unit cells of the structure of antimony thio-iodide, which has the largest known photoconductivity effect, and a number of other interesting physical

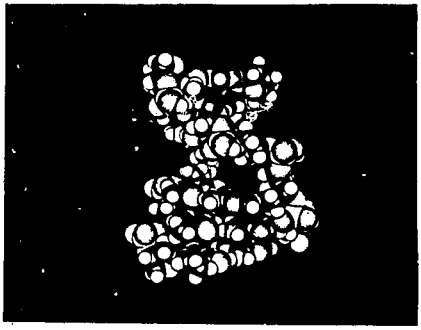

Figure 11 Six base pairs of DNA.

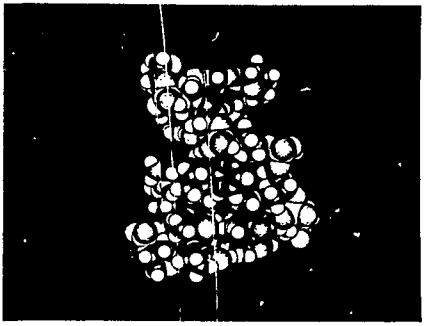

Figure 12 DNA with intercalated ethidium.

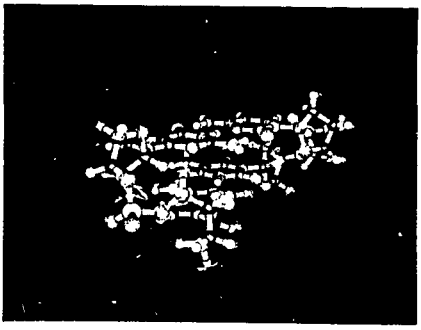

Figure 13 Double exposure.

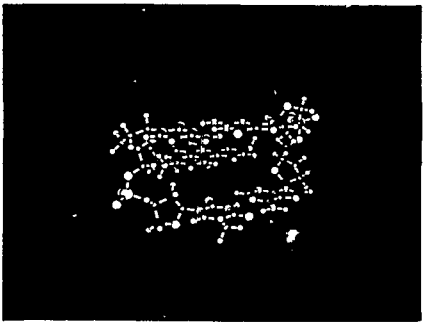

Figure 14 Ball and stick image.

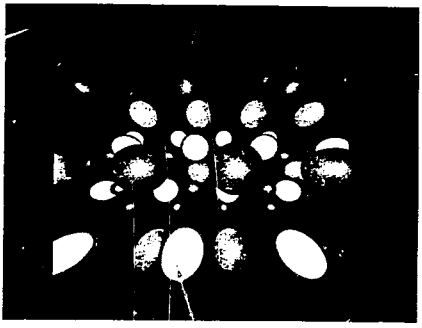

Figure 15 IMAX view of crystal.

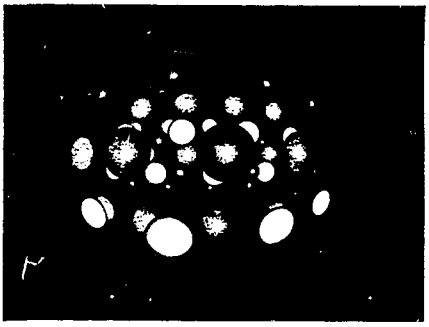

Figure 16 OMNIMAX view of crystal.

properties. If viewed from a distance of half the picture width (possible only if you are very near-sighted) the ellipses will be forshortened into circles. Figure 16 shows the OMNIMAX image of the same structure. Note that the spheres now undergo the reverse distortion.

Figure 17 shows the outlines of the visible regions of Fig. 16, as they would appear on the one-bit-video TMDS screen in a user's office.

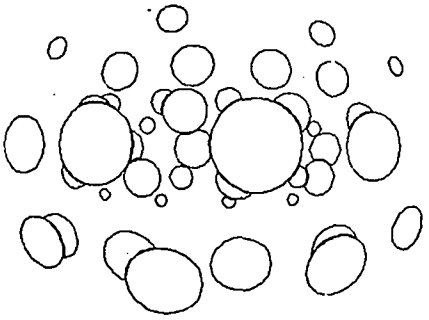

Figure 17. Outlines for Fig. 16, in one-bit video.

References

1. Blinn, James F. Models of light reflection for computer synthesized pictures. Computer Graphics Vol. 11, no. 2 (1977), pp. 192-198.

2. Bresenham, J. E. An incremental algorithm for digital display of circular arcs. Communications of the ACM Vol 20, no. 2 (1977), pp. 100-106.

3. IMAX. Promotion brochure, November 1977, available from IMAX Systems Corporation, P.O. Box 224 Cambridge, Ontario Canada N1R5T8.

4. OMNIMAX. Promotion brochure, September 1977 available from IMAX Systems Corporation, ibid.

5. Knowlton, Ken and Cherry, Lorinda. ATOMS, a three-d opaque molecule system. Computers and Chemistry Vol. 1, no. 3 (1977) pp. 161-166.

6. Max, Nelson. ATOMLLL - a three-d opaque molecule system, Lawrence Livermore Laboratory version, UCRL-52645, Lawrence Livermore Laboratory 1979.

7. Max, Nelson. ONA with ethidium. 5 minute color silent computer animated film, available on loan from the author.

8. Porter, Thomas. Spherical shading. Computer Graphics Vol 12, no. 3 (1978) pp. 282-285.

9. Staudhammer, John. On display of space filling atomic models in real-time. Computer Graphics Vol. 12, no. 3 (1978) pp. 167-172.

APPENDIX

Here are the details for approximating the ellipse of *Eq. 12* by the four circular arcs *WJ*, JL, LM, and MN, shown in Fig. 9. One of these, NJ, has center at P=(0,-D) and radius R, and another, JL, has center Q=(C,0) and radius S. If W=(X,Y) is a point on the approximation, then the "relative radial error"

$$E = \frac{X^2}{A^2} + Y^2 - 1 \qquad \ldots 13)$$

represents the radial distance from the dome projection of W to the closest point on the circle which is the projection of the ellipse. We wish to determine the four numbers C, D, R, and S, as functions of the elongation A, to minimize the absolute value of E over all points W on the approximation.

Since our shading scheme will overflow if the approximation lies outside the true ellipse, we require E to be non-positive. This makes the approximation tangent to the ellipse at eight points of two types, represented in Fig. 9 by G and H respectively. The relative radial error E is worst at eight points of two other types, represented by U and V respectively.

We can get four equations in the four unknowns C, D, R, and S, as follows. By the pythagorean theorem in triangle POQ, we have

$$C^2 + D^2 = (R-S)^2 \qquad \ldots 14)$$

since the length of the hypotenuse PQ is the difference in the radii of the two circles. Next, since the large arc is tangent to the ellipse at G, we get two equal expressions for the distance PG:

$$R = D + 1 \qquad \ldots 15)$$

Now as we continuously adjust the four parameters, keeping the two arcs tangent to each other, and to the ellipse, the two relative errors E_1 and E_2, at U and V, respectively, will change. A decrease in one will be compensated by an increase in the other. Thus the overall minimum will occur when E_1 and E_2 are equal. Now, the error E_1 at *U = (C+S,0) is easy to compute:*

$$E_1 = \frac{(C+S)^2}{A^2} - 1. \qquad \ldots 16)$$

To find the error at V, we note that V represents a local minimum of the error E along the arc GVJ. Let W=(X,Y) be a point on this arc, and e be the angle between the radius PW and the X axis. To minimize E, we express it as a function of the angle e. Along the arc GVJ, X and Y are given by

$$X = R \cos e$$

$$Y = R \sin e - D$$

Substituting in Eq. 13, we must minimize

$$E(\theta) = \frac{(R\cos\theta)^2}{A^2} + (R\sin\theta - D)^2 - 1 \quad \ldots 17)$$

which can be written in terms of sin θ alone as

$$E(\theta) = R^2\left(1-\frac{1}{A^2}\right)\sin^2\theta - 2DR\sin\theta + \frac{R^2}{A^2} + D^2 - 1 \quad \ldots 18)$$

This is a quadratic function of sine, and takes on the minimum value:

$$E_2 = \frac{R^2}{A^2} - \frac{D^2}{A^2-1} - 1 \quad \ldots 19)$$

Since the largest error is a minimum when E_1 and E_2 are equal, we combine Eqs. 16) and 19) to get

$$\frac{R^2}{A^2} - \frac{D^2}{A^2-1} = \frac{(C+S)^2}{A^2} \quad \ldots 20)$$

To find the fourth equation, note that the tangency at H occurs at the point on the arc JHU where the error E takes on its maximum value, zero. Along this arc

$$X = S\cos\theta + C \quad , \quad \text{and}$$

$$Y = S\sin\theta$$

so we have

$$E(\theta) = \frac{(S\cos\theta + C)^2}{A^2} + (S\sin\theta) - 1 \quad \ldots 21)$$

which, written in terms of cosθ alone, becomes

$$E(\theta) = S^2\left(\frac{1}{A^2} - 1\right)\cos^2\theta + \frac{2SC}{A}\cos\theta + \frac{C^2}{A^2} + S^2 - 1 \quad \ldots 22)$$

Note that the coefficient of S^2 is negative, when A 1, so this quadratic function has a maximum. Computing this maximum value and setting it to zero, we get

$$\frac{C^2}{A^2} + S^2 - 1 + \frac{C^2}{A^2(A^2-1)} = 0 \quad \ldots 23)$$

Thus, our four equations in the four unknowns are equations 14), 15), 20) and 23). These equations can be manipulated algebraically to give a single fourth degree polynomial for S, whose coefficients depend on A.

The appropriate root S of this polynomial was tabulated for 21 non-uniformly spaced values of the elongation A, from 1 towards infinity, and then approximated by a least squares fit polynomial in powers of 1/A. The result was

$$S(A) = .33333 + \frac{.62934}{A} + \frac{.06592}{A^2} - \frac{.03992}{A^3} + \frac{.01135}{A^4} \quad \ldots 24)$$

which approaches 1 when A approches 1, and approches 1/3 when A approches infinity. If A and S are known, C, D, and R can be determined from Eqs. 23), 14) and 15).